Phase diagram for area scaling in bistable hysteresis

Debashish Bose* and Subir K. Sarkar†
School of Physical Sciences, Jawaharlal Nehru University, New Delhi 110 067, India
(Received 13 June 1997)

We present a comprehensive numerical study of the scaling properties of the area of the hysteresis loop generated by the dynamics of the equation $\dot{x}(t)=x-x^3+\alpha\ \cos\omega t$. Scaling exponents of the area with respect to both amplitude (α) and frequency (ω) of modulation are calculated over a very large region of the amplitude-frequency plane and a phase diagram of the scaling properties is constructed on the basis of these data. [S1063-651X(97)03812-9]

PACS number(s): 05.45.+b, 42.65.Pc, 02.90.+p, 42.55.−f

I. INTRODUCTION

The phenomenon of hysteresis in simple model systems has received considerable attention over the last few years [1–12]. This revival of interest is due partially to its technological importance. But it has also been driven by the fundamental interest in understanding the phenomenon itself, since it is observed in a wide variety of systems in nature. In some of the systems studied hysteresis is purely dynamical in origin, whereas in some others irreversibility is caused partially by interaction with a heat bath. In this paper we will be considering a hysteretic system of the first type, which has already received some attention in the context of switching in optical and electronic devices. An example of one such work is Ref. [13], which is henceforth referred to as JGRM in this paper. The dynamical equation studied in JGRM is given by

$$\frac{dx}{dt}=ax-bx^3+\alpha\ \cos\omega t \tag{1}$$

(with a and $b>0$) where α and ω represent the amplitude and frequency of modulation. Through a suitable choice of the units of x and t, Eq. (1) can be reduced to the form

$$\frac{dx}{dt}=x-x^3+\alpha\ \cos\omega t. \tag{2}$$

In this paper we investigate the scaling properties of the area, denoted by $A(\alpha,\omega)$, of the hysteresis loop. $A(\alpha,\omega)$ is given by

$$\oint x(t)d(\alpha\ \cos\omega t),$$

where the integral is over one complete cycle of modulation after the trajectory $x(t)$ has converged onto the attractor. Scaling behavior of the quantity $A(\alpha,\omega)$ was the object of investigation in JGRM where they established, both analytically and numerically, that *in the limit of low frequency* the hysteresis loop area is given by

$$[A(\alpha,\omega)-A_0]=K[\omega^2(\alpha^2-\alpha_c^2)]^{1/3}, \tag{3}$$

where α_c (equal to $2/3\sqrt{3}$) is the critical amplitude needed for the observation of dynamical hysteresis and

$$A_0=\lim_{\omega\to 0+} A(\alpha,\omega)=1.5.$$

A_0 is independent of α for $\alpha>\alpha_c$. K is a constant of proportionality. In this paper our basic goal is to understand the scaling properties when the frequency is too high for the description given by Eq. (3) to be valid. We will present a comprehensive numerical study of the scaling properties of the area of the hysteresis loop with respect to both frequency and amplitude of modulation. This complements the study in JGRM but we have undertaken this study largely to understand our own previous results regarding hysteresis loss when noise is added to the right hand side of Eq. (2) [14]. In Sec. II we describe the methodology of our investigation. Section III describes the results and finally Sec. IV contains some concluding remarks.

II. METHODOLOGY

To study the area scaling properties of the dynamics described by Eq. (2), we make use of what is already known for the scaling properties when the dynamics is described by

$$\frac{dx}{dt}=-x^3+\alpha\ \sin\omega t. \tag{4}$$

Here the scaling law in the low frequency regime is given by

$$A(\alpha,\omega)\propto(\alpha\omega)^{4/5}. \tag{5}$$

This was derived in Ref. [15] in the context of an optically bistable semiconductor laser, when it is operated exactly at the threshold. The only difference between Eqs. (2) and (4) is the term linear in x, which is present in Eq. (2) but is missing in Eq. (4). If in the solution of Eq. (2), it so happens that x is much smaller than x^3 for most of the time in a given cycle of modulation, then in that range of parameters (α,ω) of the dynamics, scaling laws for Eq. (2) can be expected to be same as those for Eq. (4). This condition is likely to be satisfied when $\alpha\gg 1$ and ω is in an intermediate range. The reason why ω should be in an intermediate range is that the

*Electronic address: sps@jnuniv.ernet.in
†Electronic address: sarkar@jnuniv.ernet.in

amplitude of motion for a fixed value of α generally decreases with increasing ω. Thus if ω is too high the amplitude of motion is correspondingly small and the condition that x should be much less than x^3 is explicitly violated. On the other hand if ω is too small then also the argument given above for the existence of identical scaling properties breaks down. For a fixed value of α, as ω goes to zero, the hysteresis loop shrinks continuously and the size becomes arbitrarily small for Eq. (4). But, in the same limit, the area of the hysteresis loop reaches a limiting finite value for Eq. (2) with the region $x \ll x^3$ not contributing to the area of the loop at all. So if we leave out this low frequency range, where Eq. (3) should be applicable, the scaling properties for Eq. (2) should be essentially the same as those for Eq. (4) if α is sufficiently large. We keep this observation in mind in what is to follow. We have carried out extensive numerical calculation for $A(\alpha,\omega)$ in a very large range of the values of α and ω to test this proposition. Thus we find that as α goes to α_c from the upper side, the scaling exponents for both α and ω are indeed 2/3 as already derived and verified in JGRM. But as α becomes very large and ω goes beyond the low frequency regime the area scaling exponents with respect to both α and ω approach 4/5 as established in Ref. [15]. We also observe a continuous transition between these two kinds of scaling behavior in a sense that will be elaborated on through the presentation and analysis of our numerical data. We have reasons to believe that the range of amplitude and frequency that we have considered is comprehensive in the sense that no new scaling properties are expected beyond this domain in the amplitude-frequency plane.

III. RESULTS

Our numerical data are generated by integrating Eq. (2) from an arbitrary initial condition and applying suitable convergence criterion on the hysteresis loop area as a function of the cycle number of the applied modulation. Analysis of scaling of area with respect to frequency and amplitude are presented in Secs. III A and III B, respectively. Section III C combines the results of Secs. III A and III B to produce the unified phase diagram of the scaling analysis.

A. Scaling with respect to frequency

We have computed the area of the hysteresis loop as a function of frequency for a set of values of the amplitude in the range 1–10^5. For each value of the amplitude, the range of frequency studied varies from six to ten decades. Figures 1(a) and 1(b) display the area of the hysteresis loop as a function of frequency on a log-log scale for two values of amplitude for purposes of illustration. In every case, initially the area increases with frequency, reaches a maximum for a characteristic frequency $\omega_p(\alpha)$, and then decreases beyond it. For ω and α sufficiently greater than $\omega_p(\alpha)$ and α_c, respectively, the area is given exactly by $\pi\alpha^2\omega^{-1}$. This can be seen easily from Eq. (2). When α is large compared to unity and ω is sufficiently higher than $\omega_p(\alpha)$, $\dot{x}(t)$ will be equal to $\alpha \cos \omega t$ and the above result follows. In contrast, as frequency goes to zero, $[A(\alpha,\omega)-A_0]$ should go to zero as $\omega^{2/3}$. For this reason the vertical axis in Figs. 1(a) and 1(b) denotes $\log_{10}[A(\alpha,\omega)-A_0]$ and $\log_{10}A(\alpha,\omega)$ for ω less than and greater than $\omega_p(\alpha)$, respectively. As can be seen from the figures, the exponent is always -1 in the high frequency regime beyond $\omega_p(\alpha)$. For $\omega < \omega_p(\alpha)$, the situation is as follows:

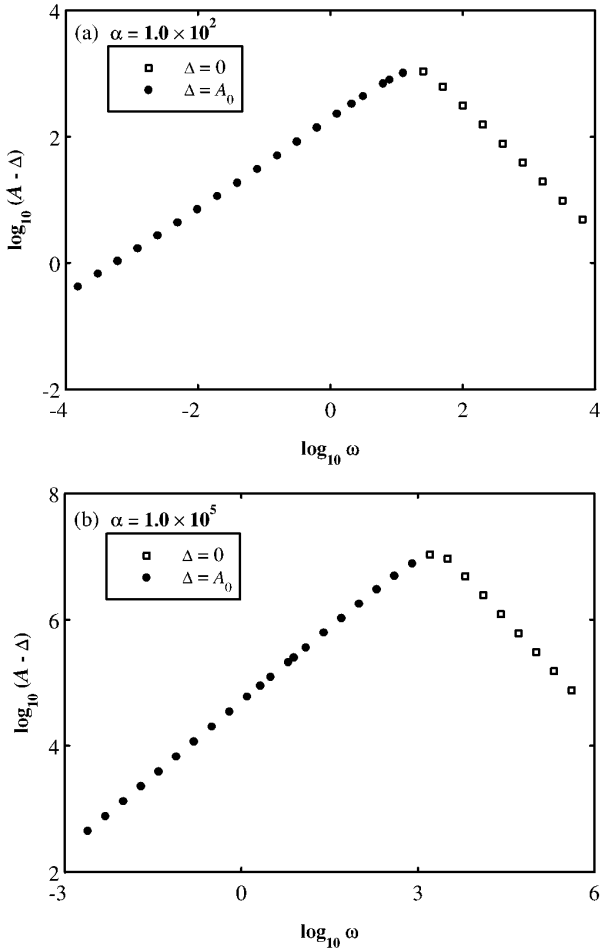

FIG. 1. Log-log plot of the area of the hysteresis loop as a function of the frequency of modulation ω for two different values of the amplitude of modulation: (a) $\alpha = 10^2$ and (b) $\alpha = 10^5$. A is the area and Δ has different values specified in the figures for points denoted by different kinds of symbols, ● and □.

$\omega_p(\alpha)$ is a monotonically increasing function of α and goes as $\alpha^{2/3}$ for $\alpha \gg \alpha_c$. As we will see later, this power law dependence of $\omega_p(\alpha)$ is consistent with the scaling behavior we are proposing and is supported by our numerical data. So in the region where area increases with frequency, the upper limit of the range of ω for a particular value of α is given by $\omega_p(\alpha)$, which is intrinsic to the problem. On the other hand, although the lower limit of ω is actually zero, for the purpose of numerical work, computational constraints force us to take its value to be in the range of 10^{-4}–10^{-3}. We denote this lower limit by $\omega_{\min}(\alpha)$. This computational limitation creates a problem when it comes to verifying the area scaling law in the limit $\omega \to 0$, for larger values of α. We expect the exponent to be 2/3 for frequency in the range between 0 and some upper limit $\omega_0(\alpha)$. But $\omega_0(\alpha)$ continues to decrease as α increases and eventually falls below the lowest frequency $[\omega_{\min}(\alpha)]$ that we can deal with computationally, within our resources. Figure 1(b) illustrates such a situation where the range with the exponent equal to 2/3 is entirely below the

TABLE I. Scaling exponents with respect to frequency and their ranges of applicability for different values of the amplitude.

Amplitude	Frequency range	Scaling exponent	Region
1.0	$10^{-3.8}-10^{-1.4}$	0.656	I
	$>10^{1.0}$	-1.000	IV
10.0	$10^{-3.9}-10^{-0.1}$	0.667	I
	$>10^{1.6}$	-0.999	IV
1.0×10^{2}	$10^{-3.9}-10^{-2.6}$	0.670	I
	$10^{-2.3}-10^{0.5}$	0.717	II
	$>10^{1.6}$	-1.000	IV
1.0×10^{3}	$10^{-3.9}-10^{-2.2}$	0.699	II
	$10^{-2.0}-10^{0.9}$	0.756	III
	$>10^{2.2}$	-1.000	IV
1.0×10^{4}	$10^{-3.9}-10^{-2.6}$	0.733	II
	$10^{-2.3}-10^{1.8}$	0.772	III
	$>10^{2.9}$	-0.999	IV
1.0×10^{5}	$10^{-2.7}-10^{2.0}$	0.784	III
	$>10^{3.8}$	-1.000	IV

lowest frequency for which the data are available. The data for frequency between $\omega_{\min}(\alpha)$ and $\omega_p(\alpha)$ are divided into one or more ranges such that data over each range can be fitted to a straight line to a very good approximation.

Table I shows the results of this analysis for a representative set of values of the amplitude. It contains information regarding the ranges into which the data have been divided in each case and the best fit value of the scaling exponent for each range. The data contained in Table I reflect the following scenario: for larger values of the amplitude there will be three regions. Region I covers the domain $0<\omega<\omega_0(\alpha)$ where the scaling exponent is 2/3. Region III, which will exist only when α is sufficiently high, is characterized by an exponent of 4/5—the domain of applicability being $\omega_1(\alpha)<\omega<\omega_{\max}(\alpha)$, where $\omega_{\max}(\alpha)$ is somewhat smaller than $\omega_p(\alpha)$. Region II $[\omega_0(\alpha)<\omega<\omega_1(\alpha)]$ is a transition region where the slope changes from 2/3 to 4/5. The region containing data with $\omega>\omega_p(\alpha)$ is defined to be region IV and it exists for all values of the amplitude. The last column of Table I displays information regarding the type of region that the data in a particular row represent. When α is just above α_c, only regions I and IV will be present. As α is increased so that $\omega_p(\alpha)$ is sufficiently higher than $\omega_0(\alpha)$, region II will also make an appearance. Finally as α increases even more region III will also come into the picture and an increasingly higher range of data just below $\omega_p(\alpha)$ will have a slope of 4/5 as α continues to increase. While checking this scenario with the data that are presented in Figs. 1(a) and 1(b) and Table I one has to remember that all or parts of regions I and II may be missing at higher amplitudes since the data in the range $0<\omega<\omega_{\min}(\alpha)$ are not available.

B. Scaling with respect to amplitude

The analysis for scaling with respect to amplitude also follows the procedure used above. For purposes of illustration the area of the hysteresis loop is plotted as a function of the amplitude on a log-log scale for the time period (T) equal to 3.2×10^{2} and 1.25×10^{-1} in Figs. 2(a) and 2(b),

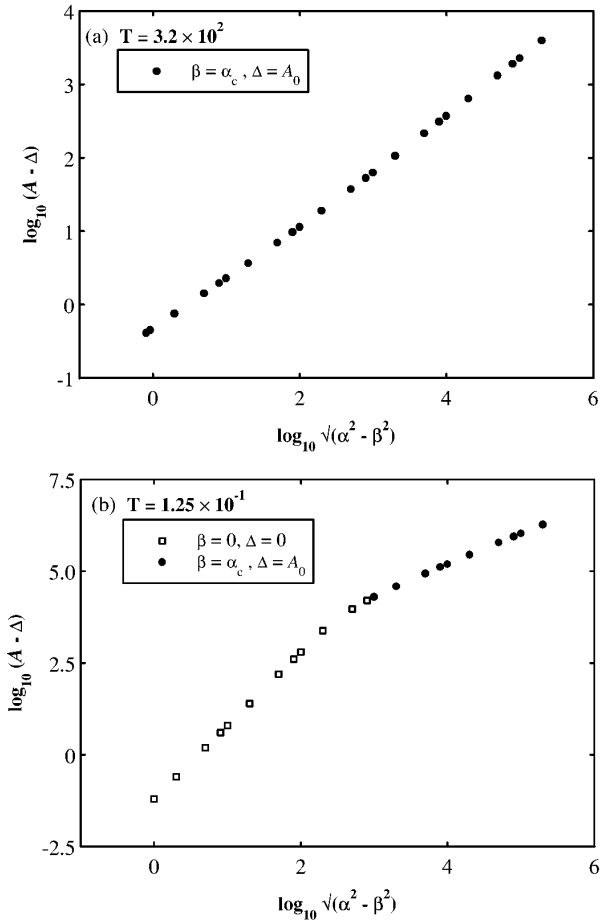

FIG. 2. Log-log plot of the area of the hysteresis loop as a function of the amplitude of modulation α for two different values of the time period of modulation: (a) $T=3.2\times10^{2}$ and (b) $T=1.25\times10^{-1}$. A is the area. Δ and β have different values specified in the figures for points denoted by different kinds of symbols, ● and □.

respectively. The analysis in the following makes use of data computed for a set of values of time period spanning seven decades. The amplitude α varies over five decades in each case. The area is always a monotonically increasing function of amplitude. To facilitate scaling analysis the data in Figs. 2(a) and 2(b) are presented using appropriate biases Δ and β for area and amplitude, respectively. The actual values of Δ and β are different for points represented by different kinds of symbols and their values are given in the figures. The points represented by squares denote cases when ω is greater than $\omega_p(\alpha)$. This is the region where area (A) is known to be proportional to $\alpha^2\omega^{-1}$ and thus for these points, defined to be part of region IV (in continuation of the notation used in Sec. III A), the slope should be 2. For the data outside of region IV we are actually plotting $[A(\alpha,\omega)-A_0]$ as a function of $\sqrt{\alpha^2-\alpha_c^2}$ on a log-log scale. Over a range of α just above α_c the scaling law given by Eq. (3) should be applicable and the slope in the log-log plot should be equal to 2/3. This is denoted by region I. If the amplitude is sufficiently high then we expect the area to be proportional to 4/5 power of amplitude. Thus, independent of the value of the frequency, the slope in the log-log plot should always be 4/5 for the region (region III) where the amplitude is sufficiently

TABLE II. Scaling exponents with respect to amplitude and their ranges of applicability for different values of the time period.

Time period	Amplitude range	Scaling exponent	Region
2.56×10^{3}	$10^{0.21}-10^{2.4}$	0.677	I
	$10^{2.6}-10^{3.7}$	0.730	II
	$10^{4.2}-10^{5.0}$	0.775	III
3.20×10^{2}	$10^{0.03}-10^{1.4}$	0.683	I
	$10^{1.9}-10^{2.9}$	0.735	II
	$10^{3.2}-10^{5.3}$	0.786	III
4.00×10^{1}	$10^{-0.06}-10^{2.0}$	0.732	II
	$10^{2.6}-10^{5.3}$	0.796	III
5.00×10^{0}	$10^{0.90}-10^{5.3}$	0.806	III
1.25×10^{-1}	$10^{0.03}-10^{2.0}$	2.000	IV
	$10^{4.2}-10^{5.3}$	0.826	III
2.44×10^{-4}	$10^{0.03}-10^{5.3}$	2.000	IV

high. When both regions I and III exist there is also a transition region (region II) where the slope changes from 2/3 to 4/5. This can be seen in Fig. 2(a). In Table II we present the information regarding the ranges into which the data have been divided in each case and the best fit value of the scaling exponent for each range. The type of region for each range is specified in the fourth column. Since $\omega_p(\alpha)$ is a monotonically increasing function, region IV will continue to shrink as the frequency goes to zero. Hence when the frequency is very low we should see regions I, II, and III as illustrated by Fig. 2(a). As frequency increases eventually region I will disappear first followed by region II. Simultaneously an increasing range of data in the lower amplitude end will appear in region IV.

C. Phase diagram of the scaling exponents

We now combine the results presented in the Secs. III A and III B to produce a unified phase diagram for the scaling exponents in the amplitude-frequency plane. This is displayed in Fig. 3. The four regions marked I, II, III, and IV are two-dimensional extensions of the nomenclature already used in Secs. III A and III B. The extended vertical lines touching the frequency axis denote the values of the frequency for which area versus amplitude data were presented in Table II. The filled circles very close to the amplitude axis denote the lowest frequency data points for each of the values of the amplitude for which the area versus frequency data were presented in Table I. The curve passing through the squares is the representation of the function $\omega_p(\alpha)$. Within a narrow band on either side of this curve in the ω-α plane there is no well-defined scaling property. In the region above the line PQR (region III) the scaling exponent with respect to both amplitude and frequency is 4/5. It should be remembered that, starting from the point Q, the lines QP and QR extend indefinitely. Below the line TS and above the curve for $\omega_p(\alpha)$, extended indefinitely towards the low frequency end, the scaling property is of the type represented by Eq. (3). This is the domain for which the scaling properties were first derived and verified in JGRM. Region II, in between the lines TS and QP extended indefinitely towards the low frequency end, is where the scaling exponent changes from 2/3 to 4/5 for both frequency and amplitude. To check that this phase diagram is consistent with the information available in Tables I and II one just has to take sections parallel to the frequency and amplitude axes of the phase diagram at the appropriate values of the amplitude and frequency, respectively. It must be remembered that a certain amount of subjectivity is involved in identifying the boundaries of region II as well as the high frequency boundary QR of region III. Finally, to see that the function $\omega_p(\alpha)$ goes as $\alpha^{2/3}$ for large α, consider the dependence of the function $A(\alpha,\omega)$ on α and ω on the two sides of the curve represented by the function $\omega_p(\alpha)$ in the (α,ω) plane. Since regions III and IV meet along this dividing line (apart from a narrow transition band) for higher values of the amplitude, the two expressions for $A(\alpha,\omega)$ must produce the same value along this line. Thus $[\alpha\omega_p(\alpha)]^{4/5}$ must be proportional to $\alpha^2\omega_p^{-1}(\alpha)$, i.e., $\omega_p(\alpha)$ is proportional to $\alpha^{2/3}$.

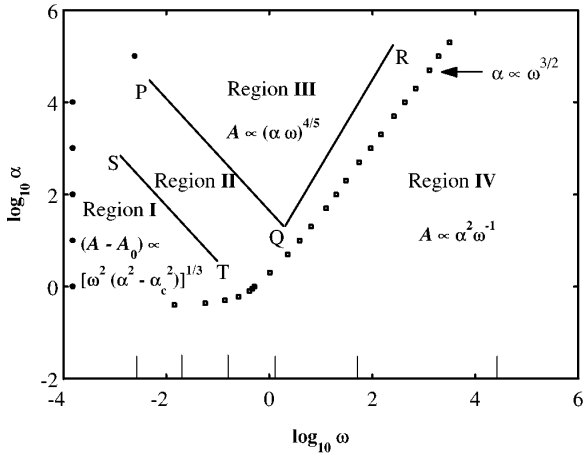

FIG. 3. Phase diagram for the area scaling properties in the amplitude-frequency plane.

IV. DISCUSSION

In this paper we have presented a comprehensive numerical study of the scaling properties of the area of the hysteresis loop generated by the dynamics of Eq. (2). For reasons that should be apparent, no new scaling properties are expected in the domains of the amplitude-frequency plane that have not been explored in this study. For the applications discussed in JGRM and in Ref. [15], hysteresis loss in the low frequency regime was the object of primary interest. But in the present study we have imposed no such restriction on the frequency. Since Eq. (2) provides a rather commonly used mathematical model of bistable hysteresis in many different kinds of situations we hope that the results described in this paper will be of relevance in these different contexts.

ACKNOWLEDGMENT

One of the authors (D.B.) acknowledges the University Grants Commission of India for financial support.

[1] G. S. Agarwal and S. R. Shenoy, Phys. Rev. A **23**, 2719 (1981); S. R. Shenoy and G. S. Agarwal, *ibid.* **29**, 1315 (1984).
[2] M. Rao, H. R. Krishnamurthy, and R. Pandit, J. Phys. Condens. Matter Lett. **1**, 9061 (1989); Phys. Rev. B **42**, 856 (1990).
[3] M. Rao and R. Pandit, Phys. Rev. B **43**, 3373 (1991).
[4] D. Dhar and P. B. Thomas, J. Phys. A **25**, 4967 (1992); P. B. Thomas and D. Dhar, *ibid.* **26**, 3973 (1993).
[5] M. Acharyya, B. K. Chakrabarti, and R. B. Stinchcombe, J. Phys. A **27**, 1533 (1994).
[6] W. S. Lo and R. A. Pelcovits, Phys. Rev. A **42**, 3973 (1990).
[7] W. Wu, B. Ellma, T. F. Rosenbaum, G. Appeli, and D. H. Reich, Phys. Rev. Lett. **67**, 2076 (1991).
[8] T. Tome and M. J. de Oliveira, Phys. Rev. A **41**, 4251 (1990).
[9] T. Zhou, F. Moss, and P. Jung, Phys. Rev. A **42**, 3161 (1990).
[10] A. Simon and A. Libchaber, Phys. Rev. Lett. **68**, 3375 (1992).
[11] M. C. Mahato and S. R. Shenoy, Phys. Rev. E **50**, 2503 (1994).
[12] V. Banerjee and S. Dattagupta, Phys. Rev. B **50**, 9942 (1994).
[13] P. Jung, G. Gray, R. Roy, and P. Mandel, Phys. Rev. Lett. **65**, 1873 (1990).
[14] D. Bose and S. K. Sarkar, Phys. Lett. A **232**, 49 (1997).
[15] A. Hohl, H. van der Linden, R. Roy, and G. H. Goldsztein, Phys. Rev. Lett. **74**, 2220 (1995).